



SRTTU

Journal of Computational and Applied Research  
in Mechanical Engineering

jcarme.sru.ac.ir

JCARME

ISSN: 2228-7922

## Research paper

## A CFD analysis of the effects of injection and suction through a perforated square cylinder on some thermo-fluid parameters

M. E. Vakhshouri\* and B. Çuhadaroğlu

Department of Mechanical Engineering, Karadeniz Technical University, Trabzon, 61080, Turkey

---

**Article info:**
**Article history:**

Received: 27/03/2020

Revised: 19/11/2020

Accepted: 22/11/2020

Online: 24/11/2020

**Keywords:**

Injection and suction,

Perforated square cylinder,

Heat transfer,

Turbulent flow.

\*Corresponding author:

[elyadv@ktu.edu.tr](mailto:elyadv@ktu.edu.tr)


---

**Abstract**

The effects of uniform injection and suction through the surfaces of a perforated square cylinder on the vortex shedding, heat transfer and some aerodynamic parameters have been investigated numerically. The finite-volume method has been used for solving the Navier-Stokes equations for incompressible and turbulent near-wake flow ( $Re \approx 21400$ ) with the  $k$ - $\epsilon$  turbulence model equations. To find the optimum conditions, the effects of injection and suction through the front surface (case I), the rear surface (case II), top-bottom surfaces (case III) and all surfaces (case IV) with various injection/suction coefficient  $\Gamma$  are studied. The results reveal that parameters such as pressure and drag coefficients and Nusselt number are influenced drastically in some cases as well as flow field parameters. For instance, the maximum reduction of the drag coefficient occurs at case IV while the maximum increase and reduction of  $Nu$  number occur at  $(|\Gamma|) = 0.025$  for all cases about 46% and 32%, 61% and 63%, 92% and 60% and 180% and 115% for cases I, II, III and IV respectively.

---

### 1. Introduction

Analysis of vortex shedding and wake region behind bluff bodies plays an important role in industrial and engineering applications such as thermal protection of high-speed systems, heat transfer enhancement in heat exchangers, drag, lift and vibration control, dynamic install, reducing acoustic effects, etc. Main problems in flow systems in such applications are flow-influenced vibrations and oscillating forces due to flow velocities. There are two methods to overcome the problem by reducing the fluctuating forces and mitigating vortex shedding. Passive and active flow control

techniques are used to design industrial structures. The passive method works by modifying the geometrical shape or attaching extra devices such as sinusoidal front and rear faces, slot flow, splitter plate, control plates and rods (e.g. [1-8]). Injection and suction through a surface, electromagnetic forces, rotationally oscillating body, bleeding through a surface, using streamwise oscillating foil and exerting an external magnetic field ([9-15]) are some examples of active methods, which work with energy input. Generating secondary flow like transpiration through perforated surfaces of a bluff body as active control of the flow field can control the characteristics of boundary layers

such as boundary layer thickening, surface skin friction and drag reduction, avoiding the separation of the boundary layer and hence preventing the transition to turbulence, etc.

Numerous papers have been published analyzing the effects of blowing from a perforated surface to the main flow. Simpson [16] reviewed the characteristics of turbulent boundary layers at low Reynolds numbers with and without transpiration. Schetz and Nerney [17] studied the turbulent boundary layer experimentally with blowing and surface roughness and reported that increasing the injection rate increases turbulence intensity in the boundary layer. Effects of mass bleeding into the flow have been experimentally investigated by Yang et al. [18]. The results reveal that the reverse horizontal velocity and flow rate, turbulence intensity, and Reynolds shear stress suppressed within the whole recirculating zone as a result of normal mass bleed. Bellettre et al. [19] analyzed the turbulent boundary layer in case of injection from a porous plate and observed an important decrease in the friction factor heat transfer coefficient by the injection rate. Hwang and Lin [20] adopted an improved Low-Reynolds number  $k-\epsilon$  model to predict the dynamic and thermal fields in the flows with uniform wall injection and suction using DNS data of channel flow. Meinert et al. [21] measured the velocity and temperature influence of foreign gas transpiration on skin friction and heat transfer. Kudriavtsev et al. [22] numerically studied external flow over a porous flat surface with cross-flow injection that suppress drag at the interface between the boundary layer and the solid wall. Bazovkin et al. [23] performed numerical simulations of low-velocity gas flow past a flat plate to analyze the intensity of micro blowing from some part of the surface. Kornilov et al. [24] numerically and experimentally investigated the characteristics of turbulent boundary layer on a flat surface with the injection of air at the expense of the resources of an external confined flow. The results show that the local surface friction coefficient decreases constantly along with the plate.

There are limited numbers of literature that studied the effects of blowing/suction from the surfaces of a bluff body on the aerodynamic parameters and heat transfer compared to a large number of papers investigating the turbulent boundary layers on perforated plates with normal injection. Hannemann and Oertel [25] simulated the development of the wake behind a

flat plate at  $Re = 200$  numerically and found that base bleeding from the plate reduces the strength of the vortex street. Ling et al. [26] numerically studied the vortex shedding over porous square cylinders subjected to suction and injection and analyzed the Strouhal frequencies. Schumm et al. [27] experimentally studied the Kármán-vortex shedding in the wake region of two-dimensional bodies and investigated different control actions, such as wake heating, base bleed and body oscillations. Mathelin et al. [28] show that the dynamic and thermal boundary layers around a circular cylinder affected strongly by blowing with the experimentally investigated study. Ling and Fang [29] numerically investigated the effects of surface suction or blowing's strength and position on the lift and drag forces and vortex structures at  $Re = 100$ . The results reveal that in some cases suction suppresses the asymmetry of the vortex wake and reduces the lift or reduces the drag force significantly. Fransson et al. [11] in an experimental study found that continuous injection and suction at moderate levels through the cylinder walls have a large impact on the surface pressure distribution, vortex shedding frequency, and the wake flow behind a porous circular cylinder. An experimental study of the effects of transpiration from a perforated surface of a square cylinder in a two-dimensional turbulent flow on some aerodynamic parameters is presented by Çuhadaroğlu et al. [30]. The results reveal that the pressure and drag coefficients affected based on the perforated surface position of and the injection rate. An effective technique was presented by Dong et al. [31] to suppress the flow-induced vibrations of bluff bodies and find that combined injection and suction reduce the fluctuating lift force. Çuhadaroğlu and Turan [32] numerically studied the turbulent flow around a square body subjected to suction/injection from different surfaces and have found that the parameters such as Nusselt number, drag coefficient and vortex shedding were affected in some cases. Çuhadaroğlu [33] studied the effects of injection/suction from a porous square cylinder on the flow field at  $Re = 21400$ . The numerical results reveal that increasing suction velocity decreases the drag coefficient while applying suction from the top/bottom body faces attenuate the vortex shedding movement. Turhal and Çuhadaroğlu [34] analyzed the effects of the surface injection from various permeable

surfaces of the diagonal and horizontal square cylinders on some aerodynamic parameters for various Reynolds numbers. Experimental results show that blowing from the top-rear, rear and all surfaces of a diagonal square cylinder reduces the drag coefficient for all Reynolds numbers. Furthermore, blowing from all surfaces of the horizontal square cylinder reduces the drag force. Çuhadaroğlu and Turan [35] analyzed the impacts of injection/suction on heat transfer over the velocity and temperature wall functions at  $Re = 21400$ . The results show that suction increases the heat transfer while blowing from the rear surface caused thermal protection. Sohankar et al. [36] investigate the impacts of uniform injection/suction from the surfaces of a square cylinder on the flow field and heat transfer at low Reynolds numbers. The study demonstrates that the optimum case happened at suction from all surfaces of the cylinder. Teimourian et al. [37] experimentally studied the effects of wake suppression by entrainment of fluid around the perforated square body on the flow structure and vortex shedding. The results show that velocity profiles and flow structure have been affected by different perforated surfaces and, as a result, wake structures have been reduced considerably.

This review shows that the effects of the injection/suction from different perforated faces of the square cylinders with different perforation rates on the heat transfer and aerodynamic parameters have not been widely analyzed at high and moderate Reynolds numbers, and limited papers are present in the literature. Thus, the objective of the present study is to investigate how suction and injection affect the drag and heat transfer in various cases. Due to the experiences from the previous studies, the effects of uniform injection through the rear surface of a square cylinder analyzed at 3.5%, 10% and 20% perforation rate (Fig. 1) to choose the optimum case and 20% perforation case have been chosen based on the reduction in the drag coefficient. The injection/suction coefficient  $\Gamma$  is defined as  $\Gamma = a \left( \frac{u_w}{u_\infty} \right)$  where  $a$  is the matching constant. Afterward, the influences of transpiration from the front, rear, top/bottom and all surfaces of the cylinder on Nusselt number and drag coefficient have been studied and for validation the achievements of this study have been compared with the experimental values.

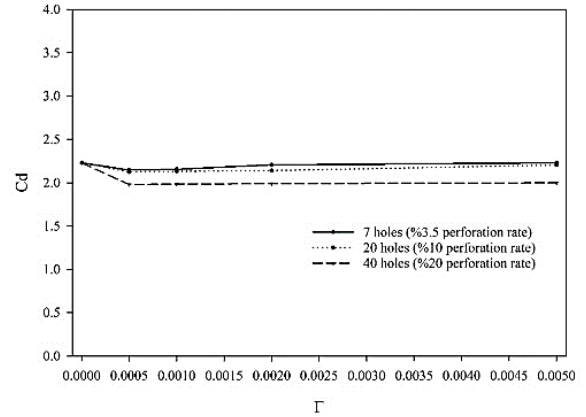


**Fig. 1.** Variation of the drag coefficient with  $\Gamma$  for injection case from the rear surface with various perforation rates.

## 2. Problem statement, numerical method and grid

This study reviews transient flow over a bluff body. Due to bulk motion in the flow field around a bluff body, the time-varying component in the wake region includes a periodic component. Turbulent fluctuations  $\phi'$  are overlying on a periodic transient motion  $\langle \phi \rangle(t)$  in the wake region of the cylinder. In the definition  $\phi(t) = \bar{\phi} + \tilde{\phi}(t) + \phi' = \langle \phi \rangle(t) + \phi'$ , instantaneous flow quantities  $\phi(t)$  include an ensemble-averaged component  $\langle \phi \rangle(t)$  (composed of a time-averaged  $\bar{\phi}$  and periodic component  $\tilde{\phi}(t)$ ) and a turbulent oscillations component  $\phi'$ . Substituting expressions of this form for the flow variables into the instantaneous continuity, momentum and energy equations and taking an ensemble average yield time-averaged Navier-Stokes and energy equations as:

$$\frac{\partial \langle u_j \rangle}{\partial x_j} = 0 \quad (1)$$

$$\frac{\partial \langle u_i \rangle}{\partial t} + \langle u_j \rangle \frac{\partial \langle u_i \rangle}{\partial x_j} = -\frac{1}{\rho} \frac{\partial \langle p \rangle}{\partial x_i} + \frac{\partial}{\partial x_j} \left[ \nu \left( \frac{\partial \langle u_i \rangle}{\partial x_j} + \frac{\partial \langle u_j \rangle}{\partial x_i} \right) - \langle u'_i u'_j \rangle \right] \quad (2)$$

$$\frac{\partial \langle T \rangle}{\partial t} + \langle u_j \rangle \frac{\partial \langle T \rangle}{\partial x_j} = \frac{\partial}{\partial x_j} \left[ \frac{\nu}{Pr} \frac{\partial \langle T \rangle}{\partial x_j} - \langle u'_j T' \rangle \right] \quad (3)$$

By using Boussinesq eddy viscosity hypothesis the Reynolds stress and heat fluxes approximate as:

$$\langle u'_i u'_j \rangle = (\nu_t) \left( \frac{\partial \langle u_i \rangle}{\partial x_j} + \frac{\partial \langle u_j \rangle}{\partial x_i} \right) - \frac{2}{3} \delta_{ij} (k) \quad (4)$$

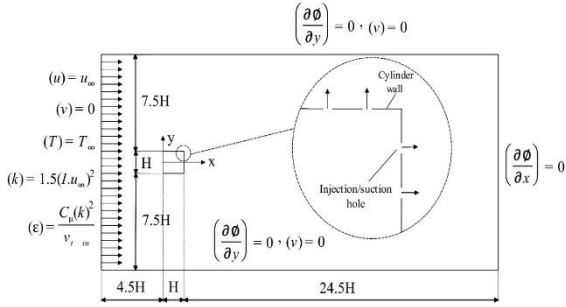


Fig. 2. Computational domain.

$$-(u'_j T') = \frac{\nu_t}{Pr_t} \frac{\partial(T)}{\partial x_j} \quad (5)$$

Standard  $k-\varepsilon$  model of Reynolds-averaged Navier-Stokes (RANS) was used for a two-dimensional flow. Turbulent energy overproduction in stagnation regions and in the small regions with high deceleration and acceleration around the square corners, which affect the vortex shedding, is a disadvantage of standard two-equation turbulence models. To produce better results, we use a modification introduced by Kato and Launder [38]. Turbulent kinetic energy production is expressed in terms of the strain rate and the vorticity based on the Kato-Launder modification. The model equations are:

$$\frac{\partial(k)}{\partial t} + (u_j) \frac{\partial(k)}{\partial x_j} = \frac{\partial}{\partial x_j} \left[ \left( \nu + \frac{\nu_t}{\sigma_k} \right) \frac{\partial(k)}{\partial x_j} \right] + P_k - (\varepsilon) \quad (6)$$

$$\frac{\partial(\varepsilon)}{\partial t} + (u_j) \frac{\partial(\varepsilon)}{\partial x_j} = \frac{\partial}{\partial x_j} \left[ \left( \nu + \frac{\nu_t}{\sigma_\varepsilon} \right) \frac{\partial(\varepsilon)}{\partial x_j} \right] + C_1 P_k \frac{(\varepsilon)}{(k)} - C_2 \frac{(\varepsilon)^2}{(k)} \quad (7)$$

$$(\nu_t) = \frac{C_\mu (k)^2}{(\varepsilon)} \quad (8)$$

$$P_k = C_\mu (\varepsilon) S \Omega$$

$$S = \frac{(k)}{(\varepsilon)} \sqrt{\frac{1}{2} \left[ \frac{\partial(u_i)}{\partial x_j} + \frac{\partial(u_j)}{\partial x_i} \right]^2}$$

$$\Omega = \frac{(k)}{(\varepsilon)} \sqrt{\frac{1}{2} \left[ \frac{\partial(u_i)}{\partial x_j} - \frac{\partial(u_j)}{\partial x_i} \right]^2}$$

In the equations above,  $S$  is the deformation tensor and  $\Omega$  is the vorticity vector. The  $k-\varepsilon$

model constants are  $\sigma_k=1$ ,  $\sigma_\varepsilon=1.3$ ,  $C_1=1.44$ ,  $C_2 = 1.92$  and  $C_\mu = 0.09$ .

Fig. 2 illustrates the schematic of the computational domain. As it can be seen, a perforated two-dimensional square cylinder with the length of  $H$  located at  $x = 0$  (Origin of the coordinate system is in the center of the front surface of the cylinder). To reduce the effects of outer boundaries, the lengths of the upstream and downstream and the width of the domain are chosen as  $4.5H$ ,  $25.5H$  and  $15H$ . These values are selected considering previous studies [32-34].

The boundary conditions of the computational domain are as follows:

(1) At the inlet:  $(u = u_\infty)$ ,  $(k) = 1.5(I.u_\infty)^2$ ,  $(\varepsilon) = \frac{C_\mu(k)^2}{\nu_{t-in}}$ ,  $(T) = T_\infty$  where the turbulence intensity ( $I$ ) is 5%. The viscosity is given by Sutherland's law with three coefficients.  $\mu = \mu_0 \left( \frac{T}{T_0} \right)^{\frac{3}{2}} \frac{T_0+S}{T+S}$  with  $T_0 = 273.11$  K,  $S = 110.56$  K, the inlet viscosity  $\mu = 1.7894 \times 10^{-5} \frac{kg}{ms}$ , the reference viscosity  $\mu_0 = 1.716 \times 10^{-5} \frac{kg}{ms}$  and the inlet temperature  $T_\infty = 373$  K.  $Re = 21400$ ,  $\rho = 1$  kg/m<sup>3</sup> and  $u_\infty = 0.38$  m/s.

(2) At the top and bottom boundaries:  $\left( \frac{\partial \phi}{\partial y} \right) = 0$ ,  $(v = 0)$ .

(3) At the outlet:  $\left( \frac{\partial \phi}{\partial x} \right) = 0$ .

(4) At the top and bottom cylinder boundaries:  $(v = v_w)$ ,  $\Gamma = a \left( \frac{v_w}{u_\infty} \right)$ ,  $(k) = 1.5(I.v_w)^2$ ,

$(\varepsilon) = \frac{C_\mu(k)^2}{\nu_{t-in}}$ ,  $(T) = T_w$  where  $v_w$  is the injection or suction velocity normal to the

boundary and the temperature of the cylinder wall  $T_w = 273$  K. Where  $\Gamma$  is the normalized injection or suction coefficient and  $a$  is the matching constant.

(5) At the front and rear cylinder boundaries:  $(u = u_w)$ ,  $\Gamma = a \left( \frac{u_w}{u_\infty} \right)$ ,  $(k) =$

$1.5(I.u_w)^2$ ,  $(\varepsilon) = \frac{C_\mu(k)^2}{\nu_{t-in}}$ ,  $(T) = T_w$  where  $u_w$  is the injection or suction velocity normal to the boundary and the temperature of the cylinder wall  $T_w = 273$  K.

**Table 1.** Grid resolution details.

Grid no.	$M \times N$	Minimum grid face area (m)	Maximum grid face area (m)	$\Gamma = 0$		$\Gamma = 0.0005$		$\Gamma = -0.0005$	
				Cd	Nu	all surfaces		all surfaces	
						Cd	Nu	Cd	Nu
I	$452 \times 322$	$4.88 \times 10^{-3}$	$1.88 \times 10^{-1}$	2.23	115	1.80	97	1.75	144
II	$552 \times 382$	$4.88 \times 10^{-3}$	$8.73 \times 10^{-2}$	2.25	117	1.81	98	1.75	146

For all simulations, the finite volume method was used based on an incompressible SIMPLE algorithm. Last squares nod-based method was selected to discretize the gradient. Pressure, momentum and energy components were discretized with second-order method while the first-order-upwind scheme was used to discretize other variables such as turbulent kinetic energy and dissipation rate. The second-order implicit scheme was used in transient formulation with a fixed time step method. To determine variables such as velocity and pressure fields, temperature, turbulence, etc. Hybrid interpolation method was used with the convergence criteria of  $10^{-6}$  in all calculations.

Increasing the perforation rate of the cylinder faces provides more suction and blowing and therefore, increases the number of nodes on the body surface. Thus, a high-resolution non-uniform grid is made in the computational domain (Fig. 3) in comparison with other papers.

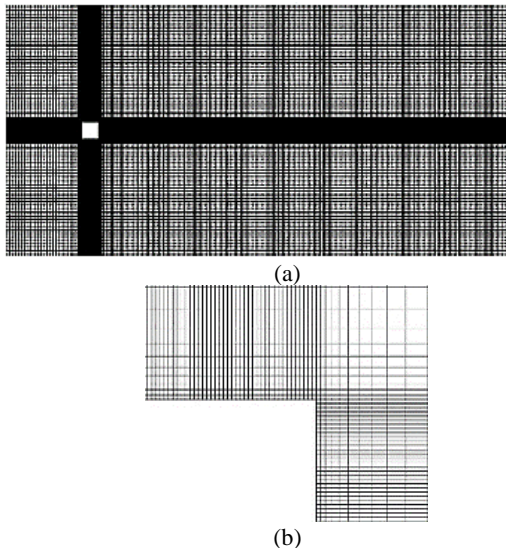


**Fig. 3.** Non-uniform computational grid ( $452 \times 322$ ): (a) whole domain and (b) enlarged view of the grid near the cylinder.

To test the effect of the grid on the results two resolutions are used for each perforation case (Table 1), and the results show that an increase of nodes has a minor influence (less than 2%) on  $C_d$  and  $Nu$ . So all simulations performed with grid I.

### 3. Results and discussion

To validate the results of this study, experimental and numerical achievements were considered as reference data to investigate the influence of uniform injection and suction through the perforated square cylinder on the flow field. Accordingly, the flow over a non-perforated square cylinder, which has been examined by Lyn et al. [39], Durao et al. [40], and Bosch and Rodi [41] and also the results achieved by Turhal and Çuhadaroğlu [34] in an experimental study of the surface injection effects on some aerodynamic parameters were considered. Moreover, experimental data by Lee [42] and Bearman and Obasaju [43] concerning turbulence effect on the surface pressure field of a square cylinder are chosen as reference data. Fig. 4 demonstrates the distribution of the time-averaged velocity component  $\bar{u}/u_\infty$  on the centreline of the cylinder at  $y = 0$ . As seen, the length of the recirculation zone matches the experimental values. In Figs. 5 and 6, the variation of drag coefficient with  $\Gamma$  for the injection cases from the rear and all surfaces of the perforated cylinder, is compared with the experimental study by Turhal and Çuhadaroğlu [34]. The figures reveal that applying injection from the rear and all faces of the body decrease the drag except the blowing case from all faces of the cylinder at  $\Gamma = 0.01$  due to pressure increase on the rear surface.

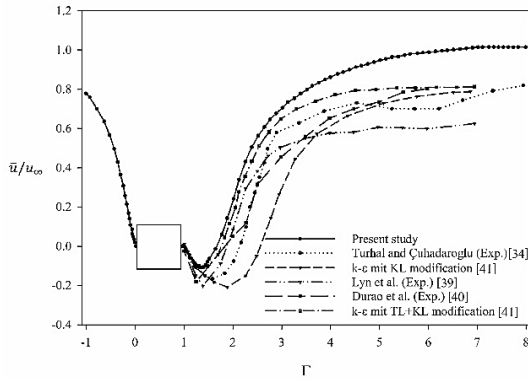


**Fig. 4.**  $\bar{u}/u_{\infty}$  on the centreline of the cylinder ( $\Gamma = 0$ ).

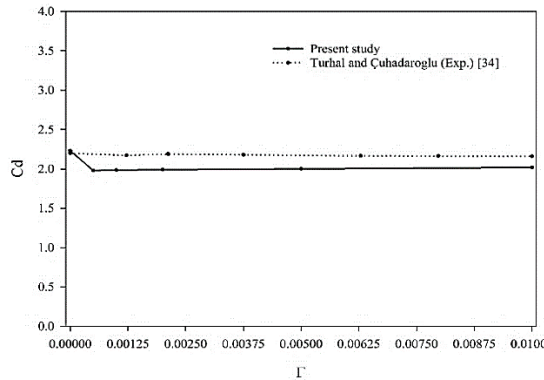


**Fig. 5.** Variation of drag coefficient with  $\Gamma$  for injection case from the rear surface.

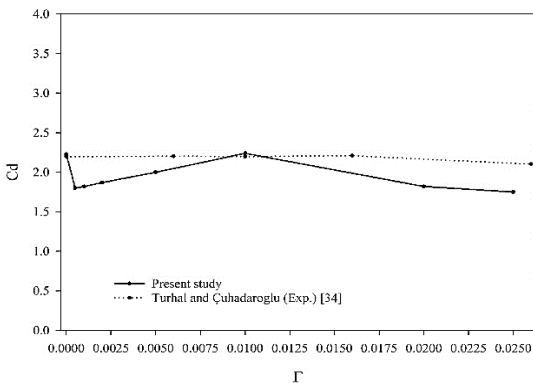


**Fig. 6.** Variation of drag coefficient with  $\Gamma$  for injection case from all surfaces.

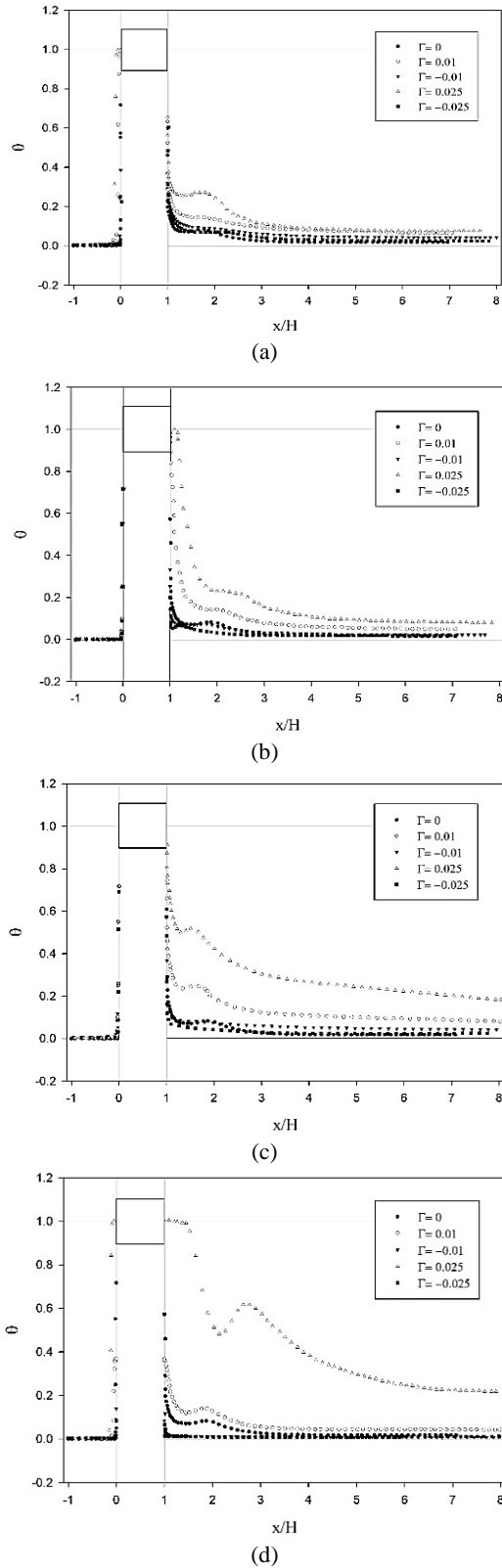
To modify the effects of injection and suction on the temperature field in the wake region and analyse the heat transfer, non-dimensional mean static temperature  $\theta$  was defined as:

$$\theta = \frac{T_{\infty} - \bar{T}}{T_{\infty} - T_w}$$

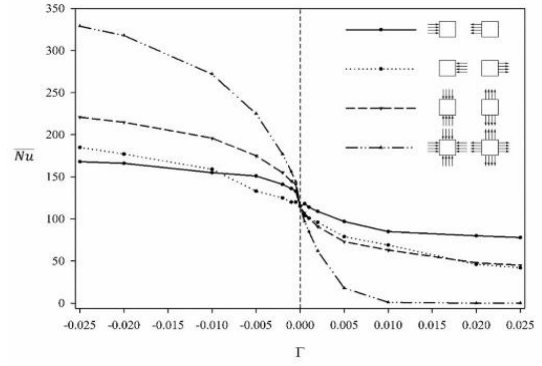
where  $T_{\infty}$ ,  $\bar{T}$  and  $T_w$  are the inlets, time-averaged and wall (injection) temperatures respectively. As seen in Fig. 7, blowing from surfaces of cylinder influences the temperature distribution on the centerline of the cylinder especially at high  $\Gamma$  whereas suction is less effective on the temperature distribution.

Fig. 8 shows the time-averaged  $Nu$  number variation with all injection and suction values. As it can be seen, by increasing suction parameter ( $|\Gamma|$ ) in all cases, time-averaged  $Nu$  number increases while on the other hand opposite behavior occurs for all injection cases. By comparing  $Nu$  number for no injection case with all other cases, it is observed that the maximum increase and reduction of  $Nu$  number occur at  $(|\Gamma|) = 0.025$  for all cases which are about 46% and 32%, 61% and 63%, 92%, 60%, 180%, and 115% for cases I (front surface), II (rear surface), III (top-bottom surfaces) and IV (all surfaces) respectively. It is also proved that applying suction through all surfaces of the cylinder provides higher heat transfer from the cylinder whereas an inverse effect happened (thermal protection) by applying injection. Fig. 9 depicted the time-averaged isotherms of injection and suction through all surfaces of the cylinder at various injection rate ( $\Gamma$ ).

The variation of the drag coefficient with  $\Gamma$  is depicted in Fig. 10. It is concluded that applying injection and suction from the front surface of the cylinder for all values of  $\Gamma$  reduces the drag coefficient. In this case, the maximum reduction of the drag coefficient is observed at  $\Gamma = -0.025$  for about 20%. Applying injection and suction through the rear surface of the cylinder reduces the drag coefficient except for values of  $\Gamma = -0.020$  and  $\Gamma = -0.025$  (S-RE-0.025) which increases the drag coefficient up to 43% and 60% respectively. Injection through top-bottom surfaces for  $\Gamma = 0.025$  (I-TB+0.025) increased of drag coefficient 57%, while for suction with  $\Gamma = -0.01$  20% decrease is seen in the drag coefficient. Generally, the figure demonstrates that suction from top-bottom faces of the cylinder reduces the drag coefficient whereas the opposite influence happened by injection. In the case of suction and blowing from all surfaces of the cylinder, for  $\Gamma = 0.01$  (I-AL+0.01) the drag coefficient is almost the same compared to no injection case.



**Fig. 7.** Nondimensional mean static temperature on the centreline of the cylinder for all blowing/suction cases: (a) front, (b) top and bottom, (c) rear and (d) all surfaces.



**Fig. 8.** Variation of mean Nusselt number with  $\Gamma$  for all injection/suction cases.

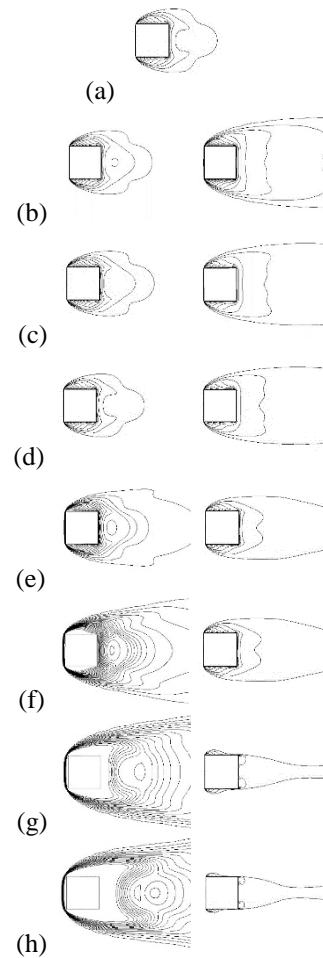


**Fig. 9.** Time-averaged isotherms of injection/suction cases through all surfaces of the cylinder: (a)  $\Gamma = 0$ ; (b)  $\Gamma = 5.0 \times 10^{-4}$ ; (c)  $\Gamma = 1.0 \times 10^{-3}$ ; (d)  $\Gamma = 2.0 \times 10^{-3}$ ; (e)  $\Gamma = 5.0 \times 10^{-3}$ ; (f)  $\Gamma = 1.0 \times 10^{-2}$ ; (g)  $\Gamma = 2.0 \times 10^{-2}$ ; (h)  $\Gamma = 2.5 \times 10^{-2}$ .

Also at  $\Gamma = -0.01$  (S-AL-0.01) a considerable decrease is observed about 40%. Furthermore,

the reduction of the drag coefficient is seen for all other values of  $\Gamma$ . Circumferential distribution of the mean pressure coefficient ( $C_p$ ) is demonstrated in Fig. 11. The results of the no-injection case yielded a fair match to experimental studies by Lee [42] and Bearman and Obasaju [43]. This figure also shows that the pressure distribution on the front surface is approximately the same for all the cases. Pressures on the other surfaces (rear, top-bottom and all) are different because of different values of  $\Gamma$ . The pressure coefficient distributions on the top and bottom surfaces are symmetric due to uniform blowing and suction for each case. Besides, the  $C_p$  curves for the cases (I-AL+0.01) and (I-TB+0.025) ensemble in shape as in cases (S-RE-0.025) and (S-AL-0.01). Fig. 11 also shows that by applying suction from the rear surface of the body with  $\Gamma = -0.025$  (S-RE-0.025), the  $C_p$  distributions on the rear face take the lowest value; while applying suction through all surfaces of the cylinder with  $\Gamma = -0.01$  (S-AL-0.01) shows the highest amount. The time average streamlines of drastically effected  $C_d$  values are depicted in Fig. 12.

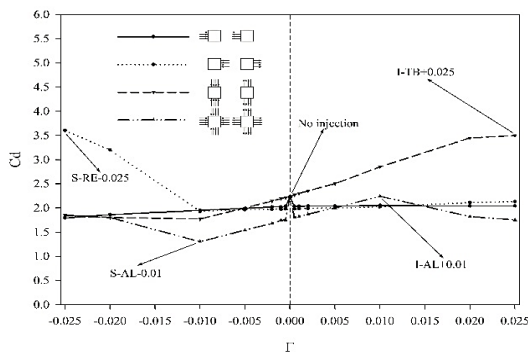


Fig. 10. Variation of drag coefficient with  $\Gamma$  for various injection/suction cases.

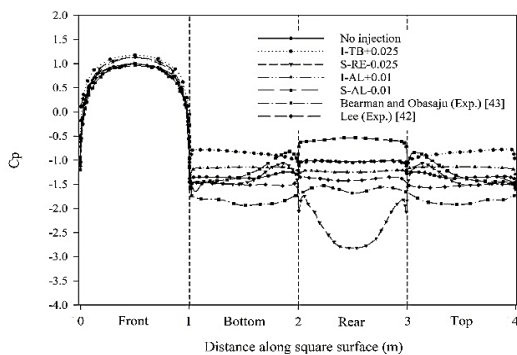


Fig. 11. Mean pressure coefficient distribution on the cylinder surfaces.

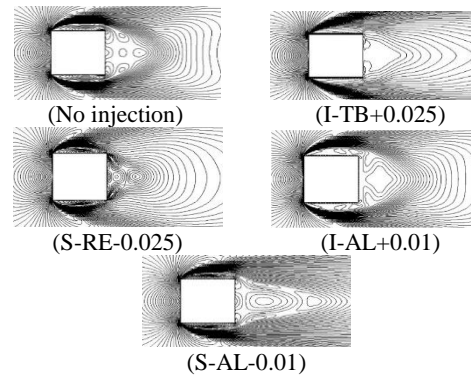


Fig. 12. Mean streamlines of some critical injection/suction cases for the drastically effected drag coefficient.

#### 4. Conclusions

The flow over a perforated square cylinder subjected to uniform surface injection/suction was studied numerically by ANSYS-FLUENT. The effects of injection/suction coefficient on the surface pressure distribution, drag and heat transfer have been investigated. It is seen that applying uniform injection/suction through the surfaces of the cylinder drastically influences the heat transfer, the drag force and surface pressure depending on the position of the perforated surface and blowing rate. The dominant effect of injection or suction on  $Nu$  number was obtained for the transpiration through all surfaces, whereas the injection/suction from the rear or front surfaces slightly influences  $Nu$  number compared to no-injection case. Suction through side surfaces may also be regarded as a heat transfer enhancement.

Numerical achievements show that the injection/suction from some faces of the cylinder body drastically affects the pressure. The pressure distribution on the rear surface was strongly influenced by the suction through all surfaces and hence the drag drastically decreased. Thus, it can be concluded that the suction with  $\Gamma = -0.01$  through all surfaces of a perforated square cylinder may be considered as a drag reduction mechanism. Additionally, it can be resulted that the suction through all surfaces of the square body is an effective way for heat transfer enhancement, whereas the injection case from all surfaces provides an efficient thermal protection.



## References

- [1] R. M. Darekar and S. J. Sherwin, "Flow past a bluff body with a wavy stagnation face", *J. Fluids Struct.*, Vol. 15, No. 3-4, pp. 587-596, (2001).
- [2] J. Y. Hwang and K. S. Yang, "Drag reduction on a circular cylinder using dual detached splitter plates", *J. Wind Eng. Ind. Aerodyn.*, Vol. 95, No. 7, pp. 551-564, (2007).
- [3] H. Hangan and J. Kim, "Aerodynamic slot-control for 2D square prisms", *J. Wind Eng. Ind. Aerodyn.*, Vol. 91, No. 12-15, pp. 1847-1857, (2003).
- [4] S. Shukla, R. N. Govardhan and J. H. Arakeri, "Flow over a cylinder with a hinged-splitter plate", *J. Fluids Struct.*, Vol. 25, No. 4, pp. 713-720, (2009).
- [5] S. Malekzadeh and A. Sohankar, "Reduction of fluid forces and heat transfer on a square cylinder in a laminar flow regime using a control plate", *Int. J. Heat Fluid Flow*, Vol. 34, pp. 15-27, (2012).
- [6] Y. Bao and J. Tao, "The passive control of wake flow behind a circular cylinder by parallel dual plates", *J. Fluids Struct.*, Vol. 37, pp. 201-219, (2013).
- [7] H. Zhu and J. Yao, "Numerical evaluation of passive control of VIV by small control rods", *Appl. Ocean Res.*, Vol. 51, pp. 93-116, (2015).
- [8] S. Malekzadeh, I. Mirzaee, N. Pourmahmoud, et al., "The passive control of three-dimensional flow over a square cylinder by a vertical plate at a moderate Reynolds number", *Fluid Dyn. Res.*, Vol. 49, No. 2, 025515, (2017).
- [9] Z. Chen and N. Aubry, "Active control of cylinder wake", *Commun. Nonlinear Sci. Numer. Simul.*, Vol. 10, No. 2, pp. 205-216, (2005).
- [10] N. Fujisawa, Y. Asano, C. Arakawa, et al., "Computational and experimental study on flow around a rotationally oscillating circular cylinder in a uniform flow", *J. Wind Eng. Ind. Aerodyn.*, Vol. 93, No. 2, pp. 137-153, (2005).
- [11] J. H. M. Fransson, P. Konieczny and P.H. Alfredsson, "Flow around a porous cylinder subject to continuous suction or blowing", *J. Fluids Struct.*, Vol. 19, No. 8, pp. 1031-1048, (2004).
- [12] A. Sevilla and C. Martínez-Bazán, "Vortex shedding in high Reynolds number axisymmetric bluff-body wakes: Local linear instability and global bleed control", *Phys. Fluids*, Vol. 16, No. 9, pp. 3460-3469, (2004).
- [13] Y. Bao and J. Tao, "Active control of a cylinder wake flow by using a streamwise oscillating foil", *Phys. Fluids*, Vol. 25, No. 5, 053601, (2013).
- [14] M. Bovand, S. Rashidi, M. Dehghan, et al., "Control of wake and vortex shedding behind a porous circular obstacle by exerting an external magnetic field", *J. Magn. Magn. Mater.*, Vol. 385, pp. 198-206, (2015).
- [15] Y. Huang, B. Zhou and Z. Tang, "Instability of cylinder wake under open-loop active control", *App. Math. and Mech.*, Vol. 38, No. 3, pp. 439-452, (2017).
- [16] R. L. Simpson, "Characteristics of turbulent boundary layers at low Reynolds numbers with and without transpiration", *J. Fluid Mech.*, Vol. 42, No. 4, pp. 769-802, (1970).
- [17] J. A. Schetz and B. Nerney, "Turbulent boundary layer with injection and surface roughness", *AIAA J.*, Vol. 15, No. 9, pp. 1288-1293, (1977).
- [18] J. T. Yang, B. B. Tsai and G. L. Tsai, "Separated-reattaching flow over a backstep with uniform normal mass bleed", *J. Fluids Eng. Trans. ASME*, Vol. 116, No. 1, pp. 29-35, (1994).
- [19] J. Bellettre, F. Bataille and A. Lallemand, "A new approach for the study of turbulent boundary layers with blowing", *Int. J. Heat Mass Transf.*, Vol. 42, No. 15, pp. 2905-2920, (1999).
- [20] C. B. Hwang and C. A. Lin, "Low-Reynolds number  $k-\tilde{\epsilon}$  modelling of flows with transpiration", *Int. J. Numer. Methods Fluids*, Vol. 32, No. 5, pp. 495-514, (2000).

- [21] J. Meinert, J. Huhn, E. Serbest, et al., "Turbulent boundary layers with foreign gas transpiration", *J. Spacecraft Rockets*, Vol. 38, No. 2, pp. 191-198, (2001).
- [22] V. Kudriavtsev, M. J. Braun and R. C. Hendricks, "Virtual experiments on drag reduction, 48th Annu. Conf. of Canadian Aeronautics and Space Inst. (CASI), 8th Aerodyn. Sec. Symp., Toronto, Canada, pp. 1-6, (2001).
- [23] A. V. Bazovkin, V. M. Kovenya, V. I. Kornilov, et al., "Effect of micro-blowing of a gas from the surface of a flat plate on its drag", *J. Appl. Mech. Tech. Phys*, Vol. 53, No. 4, pp. 490-499, (2012).
- [24] V. I. Kornilov, A. V. Boiko and I. N. Kavun, "Turbulent boundary layer on a finely perforated surface under conditions of air injection at the expense of external flow resources", *J. Eng. Phys. Thermophys.*, Vol. 88, No. 6, pp. 1500-1512, (2015).
- [25] K. Hannemann and H. Oertel, "Numerical simulation of the absolutely and convectively unstable wake", *J. Fluid Mech.*, Vol. 199, pp. 55-88, (1989).
- [26] L. M. Ling, B. Ramaswamy, R. D. Cohen, et al., "Numerical analysis on strouhal frequencies in vortex shedding over square cylinders with surface suction and blowing", *Int. J. Numer. Methods Heat Fluid Flow*, Vol. 3, pp. 357-375, (1993).
- [27] M. Schumm, E. Berger and P. A. Monkewitz, "Self-excited oscillations in the wake of two-dimensional bluff bodies and their control", *J. Fluid Mech.* Vol. 271, pp. 17-53, (1994).
- [28] L. Mathelin, F. Bataille and A. Lallemand, "Flow around a circular cylinder with non-isothermal blowing", *Exp. Therm. Fluid Sci.*, Vol. 26, No. 2-4, pp. 173-179, (2002).
- [29] G. P. Ling and J. W. Fang, "Numerical study on the flow around a circular cylinder with surface suction or blowing using vorticity-velocity method", *Appl. Math. Mech.*, Vol. 23, No. 9, pp. 1089-1096, (2002).
- [30] B. Çuhadaroğlu, Y. E. Akansu and A. O. Turhal, "An experimental study on the effects of uniform injection through one perforated surface of a square cylinder on some aerodynamic parameters", *Exp. Therm. Fluid Sci.*, Vol. 31, No. 8, pp. 909-915, (2007).
- [31] S. Dong, G. S. Triantafyllou and G. E. Karniadakis, "Elimination of vortex streets in bluff-body flows", *Phys. Rev. Lett.*, Vol. 100, No. 20, 204501, (2008).
- [32] B. Çuhadaroğlu and O. Turan, "Numerical simulation of turbulent flow around a square cylinder with uniform injection or suction and heat transfer", *Numer. Heat Transf. Part A Appl.*, Vol. 55, No. 2, pp. 163-184, (2009).
- [33] B. Çuhadaroğlu, "A numerical study on turbulent flow around a square cylinder with uniform injection or suction", *Int. J. Numer. Methods Heat Fluid Flow*, Vol. 19, pp. 708-727, (2009).
- [34] A. O. Turhal and B. Çuhadaroğlu, "The effects of surface injection through a perforated square cylinder on some aerodynamic parameters", *Exp. Therm. Fluid Sci.*, Vol. 34, No. 6, pp. 725-735, (2010).
- [35] B. Çuhadaroğlu and O. Turan, "Numerical study on heat transfer between turbulent flow and porous rectangular cylinders with uniform injection or suction", *Heat Transf. Eng.*, Vol. 33, No. 15, pp. 1232-1245, (2012).
- [36] A. Sohankar, M. Khodadadi and E. Rangraz, "Control of fluid flow and heat transfer around a square cylinder by uniform suction and blowing at low Reynolds numbers", *Comput. Fluids*, Vol. 109, pp. 155-167, (2015).
- [37] A. Teimourian, H. Hacısevki and A. Bahrami, "Experimental study on suppression of Vortex street behind perforated square cylinder", *J. Theor. Appl. Mech.*, Vol. 55, No. 4, pp. 1397-1408, (2017).
- [38] M. Kato and B. E. Launder, "The modeling of turbulent flow around stationary and vibrating square

cylinders”, *Proc. 9th Symp. Turbulent Shear Flows*, Kyoto, Japan, No. 10.4.1-10.4.6, (1993).


[39] D. A. Lyn, S. Einav, W. Rodi, et al., “A laser-Doppler velocimetry study of ensemble-averaged characteristics of the turbulent near wake of a square cylinder”, *J. Fluid Mech.*, Vol. 304, pp. 285-319, (1995).

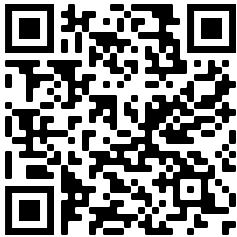
[40] D. F. G. Durão, M. V. Heitor and J. C. F. Pereira, “Measurements of turbulent and periodic flows around a square cross-section cylinder”, *Exp. Fluids*, Vol. 6, No. 5, pp. 298-304, (1988).

[41] G. Bosch and W. Rodi, “Simulation of vortex shedding past a square cylinder with different turbulence models”, *Int. J. Numer. Methods Fluids*, Vol. 28, No. 4, pp. 601-616, (1998).

[42] B. E. Lee, “The effect of turbulence on the surface pressure field of a square prism”, *J. Fluid Mech.*, Vol. 69, No. 2, pp. 263-282, (1975).

[43] P. W. Bearman and E. D. Obasaju, “An experimental study of pressure fluctuations on fixed and oscillating square-section cylinders”, *J. Fluid Mech.*, Vol. 119, pp. 297-321, (1982).

<p>Copyrights ©2021 The author(s). This is an open access article distributed under the terms of the Creative Commons Attribution (CC BY 4.0), which permits unrestricted use, distribution, and reproduction in any medium, as long as the original authors and source are cited. No permission is required from the authors or the publishers.</p>	
--	---

<p><b>How to cite this paper:</b></p> <p>M. E. Vakhshouri and B. Çuhadaroğlu, “A CFD analysis of the effects of injection and suction through a perforated square cylinder on some thermo-fluid parameters,”, <i>J. Comput. Appl. Res. Mech. Eng.</i>, Vol. 11, No. 1, pp. 23-33, (2021).</p> <p><b>DOI:</b> 10.22061/JCARME.2020.6694.1852</p> <p><b>URL:</b> <a href="https://jcarme.sru.ac.ir/?_action=showPDF&amp;article=1478">https://jcarme.sru.ac.ir/?_action=showPDF&amp;article=1478</a></p>	
--	---